

Article

Experimental Study on Ice Accretion of Aviation Jet Fuel Tube

Chengxiang Zhu ¹, Jingxin Wang ¹, Qingyong Bian ¹, Chunyang Liu ², Ning Zhao ³ and Chunling Zhu ^{3,*}

¹ Key Laboratory of Fundamental Science for National Defense-Advanced Design Technology of Flight Vehicle, Nanjing University of Aeronautics and Astronautics, Nanjing 210016, China

² Shanghai Aircraft Airworthiness Certification Center of Civil Aviation Administration of China, Shanghai 200335, China

³ State Key Laboratory of Mechanics and Control of Mechanical Structures, Nanjing University of Aeronautics and Astronautics, Nanjing 210016, China

* Correspondence: clzhu@nuaa.edu.cn

Abstract: Ice accretion on the inner surface of a fuel tube can fall off and potentially block the filters and small orifices, which thereby restricts the fuel flow to the engines during the long flying of the aircraft in cold conditions. This might cause the engines to shut down and pose a catastrophic safety threat. In this pursuit, the present study evaluates the effects of fuel temperature, entrained water concentration, and duration on the accretion of ice in flowing super-saturated RP-3 aviation jet fuel. A methodology for the quantitative mixing of water mist with fuel for accurately controlling water concentration was proposed. The different kinds of accreted ice, ‘fluffy’ and ‘pebbly’, were observed. As the distance of flow increased, a non-uniform distribution of ice on the cross-sectional area was noted. The amount of ice accretion increased with a decrease in the temperature from $-2\text{ }^{\circ}\text{C}$ and $-12\text{ }^{\circ}\text{C}$, and with an increase in entrained water concentration. Besides, the amount of ice accretion showed an increasing trend as time went on and became stable after 2 h. Our experimental results can assist to gain a better understanding of the ice accretion process in flowing super-saturated fuels and may serve as a basis for the design of the aircraft fuel system and airworthiness certification.

Keywords: ice accretion; fuel tube; airworthiness



Citation: Zhu, C.; Wang, J.; Bian, Q.; Liu, C.; Zhao, N.; Zhu, C.

Experimental Study on Ice Accretion of Aviation Jet Fuel Tube. *Aerospace* **2023**, *10*, 22. <https://doi.org/10.3390/aerospace10010022>

Academic Editor: Phil Ligrani

Received: 20 November 2022

Revised: 19 December 2022

Accepted: 22 December 2022

Published: 26 December 2022



Copyright: © 2022 by the authors. Licensee MDPI, Basel, Switzerland. This article is an open access article distributed under the terms and conditions of the Creative Commons Attribution (CC BY) license (<https://creativecommons.org/licenses/by/4.0/>).

1. Introduction

The presence of water in the aviation jet fuel has been a topic of concern for the aviation industry since this contaminating water may freeze during the long flights at high altitude and potentially possess a serious safety threat [1]. The Air Accidents Investigation Branch (AAIB) indicated the reason for the Boeing 777 crash landing at Heathrow airport in January 2008 was a sudden and non-instructive drop in fuel flow during approach, due to a restriction on the face of fuel-oil heat exchanger (FOHE) induced by the release of accreted ice. Following the investigation, the AAIB made recommendations to European Aviation Safety Agency (EASA) and Federal Aviation Administration (FAA) for further research on the aspect related to the formation mechanisms and properties of water/ice in fuel, as well as the accretion and release mechanisms of ice [2].

Aviation fuels are known to contain small quantities of dissolved water, which may precipitate gradually when the fuel is cooled [1]. Lao et al. observed that the excess dissolved water precipitated and appeared in the form of fine droplets or ice particles when the fuel was cooled down [3,4]. Murry et al. found that the micron sized water droplets immersed in JetA-1 fuel existed in a metastable sub-cooled state to around $-36\text{ }^{\circ}\text{C}$ [5]. Lam et al. made similar observations for tiny water droplets that precipitated from the fuel model (Toluene) which could maintain a metastable super-cooled state to temperature below $-30\text{ }^{\circ}\text{C}$ [6]. The supercooled water droplets could remain liquid state in cold fuel, but that hardly happened in an actual fuel system due to other impurities.

Undissolved water can also freeze to form ice crystals that may be capable of plugging the fuel filters [1]. Lao et al. observed that a substantial layer of two different types of

deposition on the sub-cooled surface seemed to grow directly from dissolved phase, in accordance with the Bergeron process [3]. Lam et al. found that the mass transfer from the metastable ice particles changed to hexagonal ice particles and attributed this phenomenon to the augmented Wegener–Bergeron–Findeisen (WBF) process and the Ostwald ripening process [6]. Lam et al. described that the accreted ice was akin to fresh snow and exhibited soft and fluffy attributes [7]. The accreted ice in a static fuel was available to understand the icing mechanism.

In order to simulate the real fuel system, a series of tests were designed to mimic the fuel flow and ice accumulation. The accreted ice found in the AAIB tests was found to be soft and mobile [2]. The release of the accreted ice in the fuel system could clog the FOHE, thereby threatening flight safety. Maloney et al. [8,9] tested accreted ice of the saturated fuel flowing through the cold pipe and observed two types of ice accumulation due to temperature differences between the fuel and pipes. Schmitz et al. [10] observed that the soft ice accreted upon the aluminum wedge block, but a large fraction of it shed off at fuel temperature below $-20\text{ }^{\circ}\text{C}$, which was considered to be a consequence of the changing ice properties and adhesion strength. Lam et al. [11] obtained accreted ice with a large porosity for super-saturated fuel, which was mixed with water at $5\text{ }^{\circ}\text{C}$. Besides, the adhesion of accreted ice, especially soft ice, was sensitive to fuel temperature. Lam et al. [7] measured the adhesion of accreted ice on horizontal and vertical sub-cooled surfaces immersed in jet fuel. Maloney et al. [9] observed the ice accumulation at $-7\text{ }^{\circ}\text{C}$, especially at the weld position. However, the accreted ice was almost invisible at $-19\text{ }^{\circ}\text{C}$. AAIB observed a critical icing temperature, called the ‘sticky’ range, between $-5\text{ }^{\circ}\text{C}$ and $-20\text{ }^{\circ}\text{C}$ [2]. Although the accreted ice in fuel pipes has been studied, there were differences owing to different fuels of varied chemical composition [12]. Thus, the test data were insufficient, especially for super-saturated low-temperature fuel.

The icing of the aircraft fuel system is a complex process. The methods of mixing water with fuel and regulating water concentration still need to be improved. The experimental data on the characteristics of accreted ice for different types of cold fuels are yet not fully understood. In this pursuit, the main objective of this study was to gain a further understanding of the ice accretion for super-saturated fuel, and the effects of test-period, fuel temperature, and entrained water concentration.

2. Experimental Methods

2.1. Experimental Principle

A schematic representation of the test rig employed for this study is shown in Figure 1. The circular fuel flow was fed from a welded SST tank of 200 L capacity and driven by a gear pump. The data acquisition system monitored the flow volume and temperature of the fuel. The former was controlled by a regulating valve and the latter was cooled by a chilling system that sprayed the liquid nitrogen into the environment chamber.

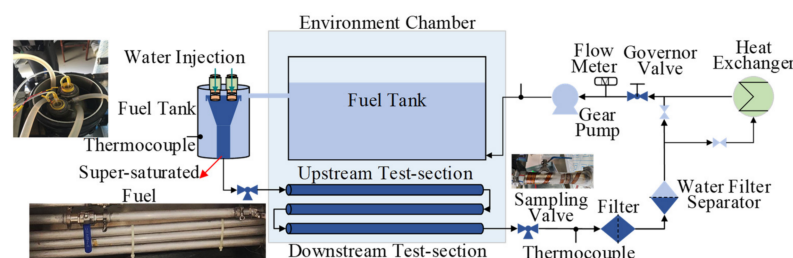


Figure 1. Schematic representation of the icing test rig. (Dark blue indicates supersaturated fuel, and light blue indicates saturated fuel).

The key component of the apparatus was the device that mixed the quantitative water mist with the fuel, as shown in Figure 2. The fuel was evenly mixed with atomized micron water droplets to achieve precise control of entrained water concentration. The device comprised mixing pipes and water atomizers with vibrating micro tapered apertures. The

water atomizers facilitated the dispersal and mixing of the water mist added quantitatively to cool fuel. The fuel surged into the mixing pipes from the surface rectangular holes. The hot water was provided by the impeller pumps for heating the wall to prevent ice formation around the holes. The super-saturated cool fuel exited the device and entered the external pipework.

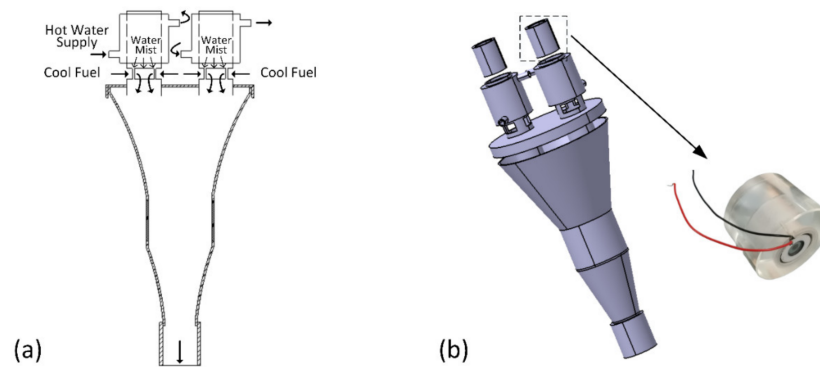


Figure 2. Device for quantitative mixing of water mist and fuel. (a) the schematic representation, (b) the 3D model.

The atomizer was composed of a water storage tank and a piezoelectricity sheet. The water was pushed by an external micro syringe pump. The water droplet dripped on the piezoelectricity sheet was rapidly atomized. The required flow volume of water was regulated according to the fuel flow rate and power of the piezoelectricity sheet:

$$M = V(\gamma_{TS} + C - \gamma) \quad (1)$$

where M is the flow volume of water (L/h), and V is the flow volume of fuel (L/h), and C is the constant for water mist loss. γ and γ_{TS} is the water concentration of saturated fuel and fuel in the test section (ppm), respectively.

The external connecting pipes (SST) were thermally insulated with rubber plastic cotton. Especially, the sampling valve before the test sections was heated by an electro-thermal film, to avoid icing leading to the uncertainty of entrained water concentration in fuel through the test section. The test loop (Aluminum, total length 21 m) was located in the environmental chamber, including two removable test sections (inner diameter 38.1 mm, length 0.6 m) at the inlet and outlet. The fuel pipes were used to observe and measure the accreted ice. After that, the filter sieved the impurities and the snow shower carried in fuel from upstream processes. Subsequently, the super-saturated fuel flowed into the water separator that was filled by the water absorbing resin, which could absorb the undissolved water and maintain the fuel saturated at low temperatures. The heat exchanger regulated the temperature of fuel, by controlling the mixing ratio of heated fuel to cool fuel in the main pipeline. In the end, the saturated fuel was driven back to the saturated fuel tank by the gear pump. The average water concentration of fuel was determined by Karl Fischer titration using the sampling valves. The experimental conditions were summarized in Table 1.

Table 1. Experimental Conditions on ice accretion of aviation jet fuel pipe.

| Test Period t (min) | Fuel Temperature T_f (°C) | Water Concentration γ_{TS} (PPM) | Fuel Flow Volume V (L/h) |
|--------------------------|--------------------------------|---|-------------------------------|
| 60 | −12 | 200 | 600 |
| 90 | −12 | 200 | 600 |
| 120 | −2, −9, −12, −15 | 150, 200, 300 | 600 |
| 150 | −12 | 200 | 600 |

2.2. Experimental Process

The tank was filled with 150 L of RP-3 aviation jet fuel. The typical temperature and water concentration profile were shown in Figure 3. The initial fuel circulated for about 0.5 h at room temperature in order to filter out the impurities and undissolved water. Subsequently, the liquid nitrogen was sprayed into the chilling chamber. The flowing fuel and pipe were cooled to a target fuel temperature. The temperature was maintained for 2 h. Based on the current flow volume, and water concentration of saturated fuel at the target temperature, the flow volume of water was determined by Equation (1). The water was added by the device for quantitative mixing of water mist and fuel. As the experiment continued, the fuel samples were taken and measured every half hour to validate that the required entrained water concentration of fuel at the inlet of test loop was steady. After the specific test period, the system was stopped, and the test section was detached. After the fuel inside the test section was drained, the weight of the test section was measured and used to quantify the ice accretion. The average value was obtained to eliminate the uncertainty in mass measurement. The test section was photographed to record the accreted ice. The whole procedures, including weight measurement and photography, was completed in the chilling chamber to prevent the influence from ambient. The ice suspended in the fuel was drained with fuel together, which was not counted in the accreted ice mass in the fuel pipe. Subsequently, the test sections were re-installed and the volume flow was increased slowly to $V = 1000$ L/h. The heat exchanger was fully opened to heat the fuel. Besides, the drain valve was opened to release the part of the free water, and the water-absorbing resin was replaced.

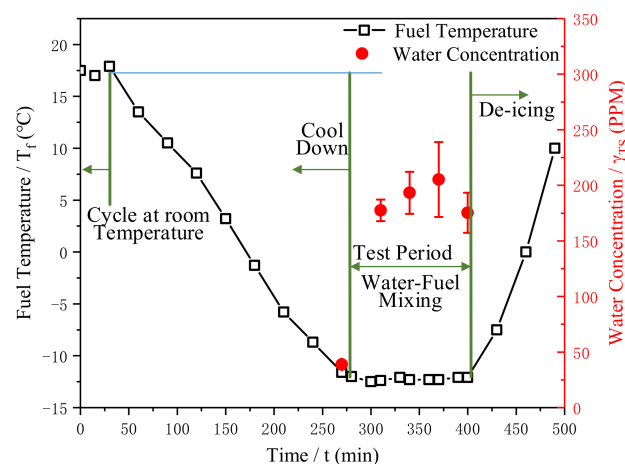


Figure 3. A typical fuel temperature and water concentration profile.

3. Results and Analysis

The icing tests methods and procedures followed in aircraft fuel systems have been reported, including under emergency conditions, which mixed large amounts of water [13–15]. The icing experiment carried out with super-saturated fuel was meaningful in the aircraft fuel system design and airworthiness certification technology. For super-saturated low-temperature fuel, the influence of the test duration, fuel temperature, and water concentration on accreted ice mass was discussed.

3.1. Influence of Duration

Considering that the test sections were located in a closed environment chamber, it was impossible to directly observe the ice accretion process. Following the procedure described above, experiments were carried out at different duration ranging from $t = 1$ h to $t = 2.5$ h. Figure 4 illustrates the ice accreted in the test sections at different durations.

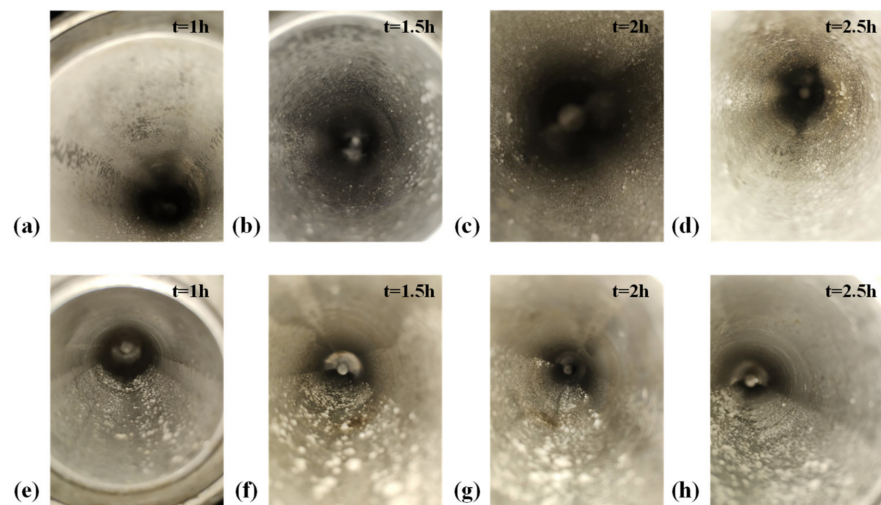


Figure 4. Ice accretion in the test-sections at different duration for $T_f = -12\text{ }^\circ\text{C}$, $\gamma_{TS} = 200\text{ ppm}$, $V = 600\text{ L/h}$. (a–d) are the ice accretion at upstream test section and (e–h) are the ice accretion at downstream test section.

Visualization of the ice accretion on the inner wall of the test sections was carried out. There were at least two different types of depositions, of which one was soft and fluffy near the wall, like frost, which seems to be similar to the ice described in related literature [3,7,10]. The other was hard and took on a ‘pebbly’ appearance. The character of accreted ice was closely related to the way of mixing water with fuel. The water mist was injected into cold fuel, resulting in rapid cooling and ice nucleation of tiny droplets. Thus, in this study, the entrained water in the fuel before entering the test loop included micron-sized supercooled water droplets and ice crystals. They collided with cold walls and froze to create the ‘pebbly’ ice. However, the thin layer of soft ice was considered to form at the cooling stage. The pipe and flowing fuel were cooled simultaneously. The entrained water was precipitated due to the decrease in fuel temperature. Although the water filter separator filtered out most of the dissolved water, the fuel began to cool down once entering the test coil. The entrained water formed the ice particles, which are sticky. With successive impingement of ice particles, a soft ice layer is formed.

It was found that the accretion level exhibited a gradual non-uniformity on the cross-sectional area with the distance of flow. The ‘pebbly’ ice in the rear test section was larger and concentrated in the lower part. Similarly, Lam et al. observed that the distribution of ice accretion was uneven in the longitudinal and circumferential directions of the fuel pipework [11]. It was seen that the micro-sized water droplets slowly fell through fuel under the effect of gravity. The settling rate is given by Stokes’ Law, which could describe the terminal velocity of the water droplets, as shown in Equation (2) [16].

$$v = \frac{(\rho_w - \rho_f)gd^2}{18\mu_f} \quad (2)$$

where v is the falling velocity of droplets in the fuel (m/s), d is the diameter of the droplets (m), and μ_f is the dynamic viscosity of fuel (NS/m^2). ρ_w and ρ_f denote the density of water and fuel (kg/m^3), respectively.

Since the size of water droplets in the super-saturated fuel was less than $50\text{ }\mu\text{m}$, and the density difference between water and fuel was comparatively modest, the settling rate of water droplets was estimated to be less than 0.12 mm/s , which could be negligible compared with the fuel flow velocity. The water droplets and ice crystals suspended in the fuel evenly adhered to the inner wall, so the ice distribution was relatively uniform in the upstream test section. With fuel flowing downstream, the water droplets/ice particles could collide and merge with each other. In addition, the accreted ice could be washed

off downstream due to its soft and mobile characteristics. In the downstream test section, the volume of ice crystals, water droplets, and accreted ice gradually increased, making it difficult to be suspended, which resulted in the non-uniform distribution of accreted ice.

The quantity of accreted ice in the upstream test section at different test duration was shown in Figure 5. For various icing conditions, tests were carried out in triplicate and the average value was obtained to eliminate the uncertainty. The results showed that with the extension of the test duration, the amount of ice accretion appeared to an increasing trend and became stable after 2 h. In this study, the undissolved water was entrained by low-temperature fuel and impacted on cold wall under the action of velocity profile, leading to ice accumulation and subsequent adsorption. Without considering the complex interface of porous media, the wall shear strength increased with the average spatial flow velocity. Prolonging the test duration, the water droplets/ice particles continuously adhered to deposition within the test loop. Meanwhile, the initial thin layer of soft ice was gradually filled with tiny water droplets and ice crystals. As the amount of accreted ice increased, the average spatially flowing velocity increased. The shear strength increased and gradually overcame the ice adhesion strength. After the equilibrium state was reached, the accreted ice no longer increased significantly. Lin et al. [17] believed that most accreted ice accumulated over a short period of time (generally less than 3 h).

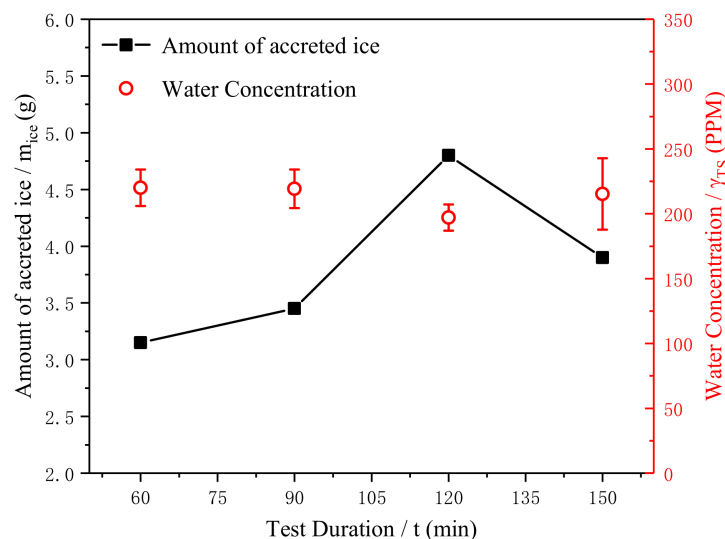


Figure 5. Mass of accreted ice in the upstream test section versus the test durations.

In order to more clearly clarify the relationship between the amount of icing and the test durations, the water concentration of the fuel samples at the inlet and outlet of the test loop were compared, as shown in Figure 6. The results suggested that the water concentration at the inlet is relatively steady, which demonstrated the initial water concentration was repeated and controlled. However, the water concentration at the outlet changed drastically. This was because the sampled fuel at the outlet was mixed with ice. The water concentrate was analyzed following the Karl Fischer method after sampled fuel was restored to room temperature, leading to a large error bar.

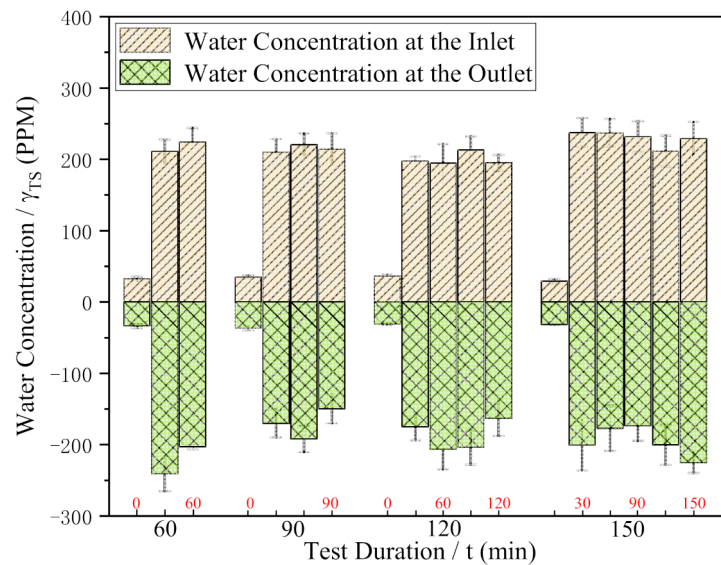


Figure 6. Water concentration of the fuel sample at the inlet and outlet of the test loop.

3.2. Influence of Fuel Temperature

From the experiments, it was found that the amount of ice accretion in the fuel pipeline reached the maximum at around 2 h. Experiments were carried out at different fuel temperatures ranging from $T_f = -2\text{ }^\circ\text{C}$ to $T_f = -15\text{ }^\circ\text{C}$. Figure 7 showed the adhered ice accretion to the inner surface of the test sections at variable temperatures.

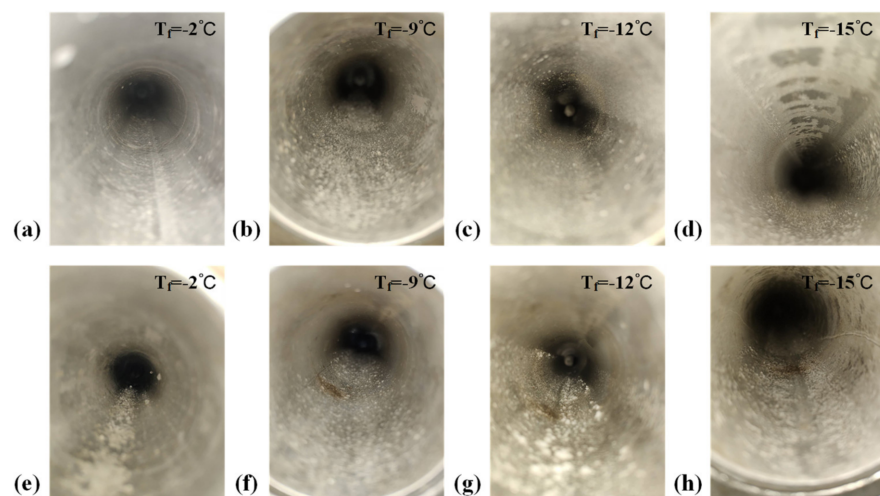


Figure 7. Ice accretion in the test sections at different fuel temperatures at $t = 2\text{ h}$, $\gamma_{TS} = 200\text{ ppm}$, $V = 600\text{ L/h}$. (a–d) are the ice accretion at upstream test section and (e–h) are the ice accretion at downstream test section.

The accreted ice was sticky and adhered to the inner wall at a fuel temperature range between $-2\text{ }^\circ\text{C}$ and $-15\text{ }^\circ\text{C}$. According to the AAIB investigations, the highest stickiness was found at around $-12\text{ }^\circ\text{C}$ [2]. It was noted that when the fuel temperature was maintained at $-2\text{ }^\circ\text{C}$, there was a little accreted ice in the upstream test section. This was consistent with the ‘sticky’ temperature region in the literature [2,10]. However, the ‘pebbly’ ice still appeared at the bottom of the downstream test section. This was because the ‘sticky’ temperature region was mainly for soft ice characteristics, while ‘pebbly’ ice is formed by larger water droplets/ice particles. The properties of ice, such as adhesion strength and porosity, were different.

The amount of the accreted ice in the upstream test section changed with the fuel temperature, as shown Figure 8. With the decrease in the fuel temperature, the mass of

accreted ice presented an increasing trend between $-2\text{ }^{\circ}\text{C}$ and $-12\text{ }^{\circ}\text{C}$, while the accreted ice occurred to fall off partly at $-15\text{ }^{\circ}\text{C}$. Schmitz et al. [10] believed that the increase of accreted ice was partly attributed to decreasing water solubility with fuel temperature.

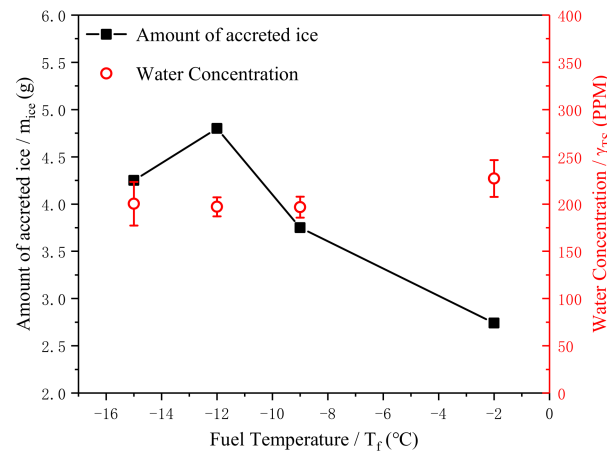


Figure 8. Mass of accreted ice in the upstream test section versus the fuel temperature.

Figure 9 illustrates the relationship between the saturated water concentration and temperature of RP-3 aviation jet fuel:

$$\gamma = 54.261e^{0.0297T_f} \quad (3)$$

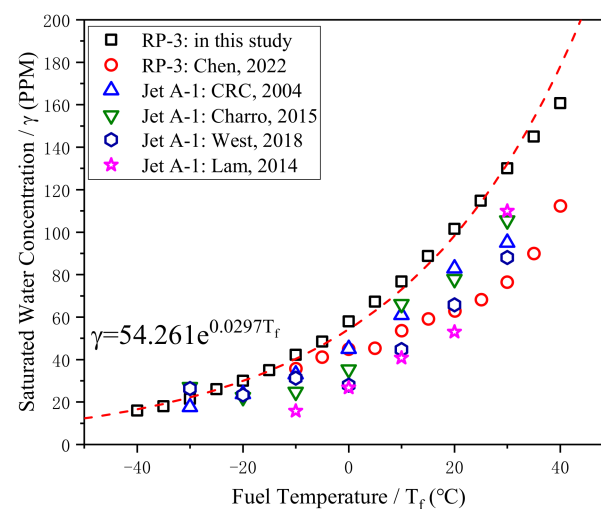


Figure 9. The saturated water concentration of fuel temperature. The red line represented the fitting line of experimental data in this study. Other experimental data were from literature [1,15,18–20].

The experimental results in this work proved consistent with those reported in the previous literature [1,15,18–20]. The deviation is attributed to the different chemical composition. The results showed that with the decrease in fuel temperature, the saturated water concentration decreased. That explained the source of the entranced water at the cooling stage. However, most of the accreted ice mass belonged to ‘pebbly’ ice in the above experiments. Thus, the influence of the dissolved water could be neglected for the super-saturated low-temperature fuel used for the experiments.

The increase in accreted ice could be attributed to two aspects: nucleation rate and ice adhesion strength. Firstly, the presence of supercooled water droplets was the precondition of nucleation and ice formation. Gibbs free energy [21] must be overcome for ice to be formed from water. The fuel temperature could be assumed as the supercooled

water temperature. Whether homogeneous or heterogeneous nucleation, the difference in Gibbs energy decreased with increases in the supercooled degree of water droplets. Thus, the frozen fraction of droplets entrained in the fuel increased with the decrease in fuel temperature.

Besides, the adhesion strength of accreted was sensitive to temperature [9]. It was agreed that the adhesion strength of ice to arbitrary substrates increases with the decrease in temperature [22]. The pipe wall temperature in the test section was cooler than the fuel temperature. Thus, the adhesion strength of ‘pebbly’ ice increased with lower wall temperature, leading to more ice particle deposition. However, when the fuel temperature is near the edges ‘sticky’ temperature region, the ice accumulation is less [9].

In this study, at a fuel temperature below $-15\text{ }^{\circ}\text{C}$, part of the accreted ice was observed to fall off, as shown in Figure 7d,h. It is noted that the shed part is the soft ice at the pipe top. This phenomenon is consistent with the results in the literature [10]. Archer et al. found that the damping effect in the thin liquid-like layer between ice and structural solid disappeared after a certain temperature [23]. The shed ice would flow backward with the fuel, potentially clogging other parts. In fact, during tests, the coarse filter was often blocked due to ice accumulation, leading to flow fluctuations.

3.3. Influence of Water Concentration of Fuel

AAIB proposed that it was difficult to control water concentration of supersaturated fuel, and the uneven distribution characteristic was one of the reasons for the limitation of the tests [2]. The cloudy or milky appearance, due to the presence of the entrained water, made it difficult to directly observe the process of icing on the solid wall in the super-saturated fuel.

Following the procedures described above, experiments were carried out at different entrained water concentration ranging from $\gamma_{TS} = 150\text{ ppm}$ to 300 ppm . Figure 10 illustrated the ice accreted in the test sections at different water concentrations.

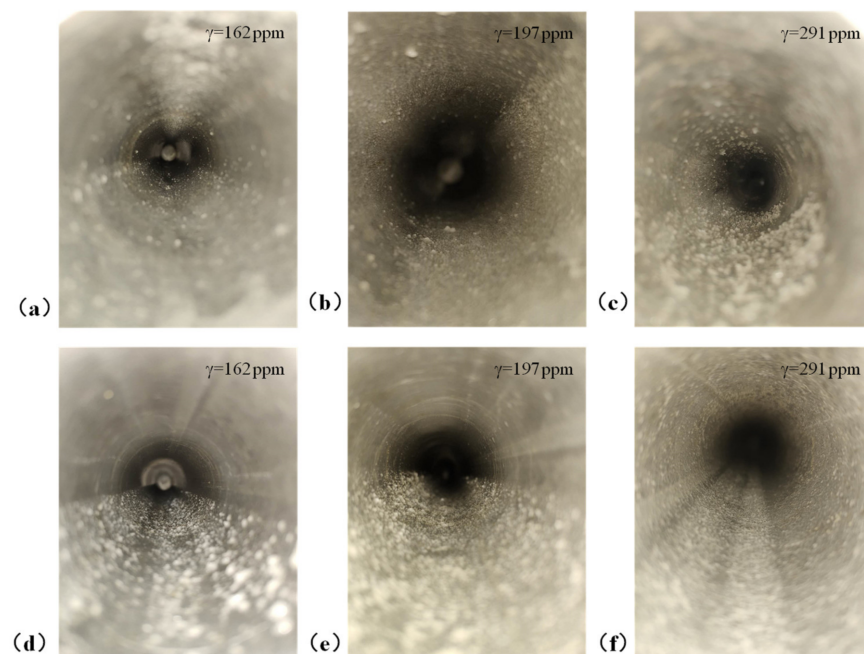


Figure 10. Ice accreted in the test-sections at varied water concentrations for $t = 2\text{ h}$, $T_f = -12\text{ }^{\circ}\text{C}$, $V = 600\text{ L/h}$. (a–c) are the ice accretion at upstream test section and (d–f) are the ice accretion at downstream test section.

In this study, the water concentration of cooled super-saturated fuel was controlled by the quantitative mixing of water mist with fuel. Figure 11 showed the comparison of the

theoretical and experimental values in the fuel samples. It was considered that the method of injecting was reliable and the water concentration was controllable.

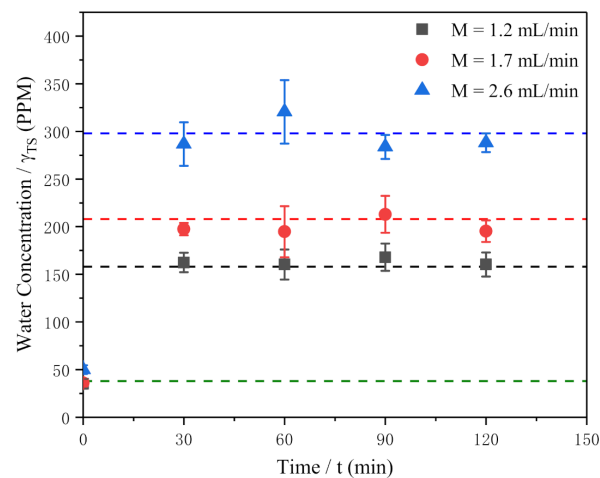


Figure 11. Comparison of theoretical and measured water concentration in the fuel samples. The spot lines represented the theoretical values.

The amount of ice accretion increased with the water concentration, as shown in Figure 12. This was because the frozen fraction of droplets increased with the increase in water concentration. More free water in fuel presented nucleation, icing, and adhering to the inner wall.

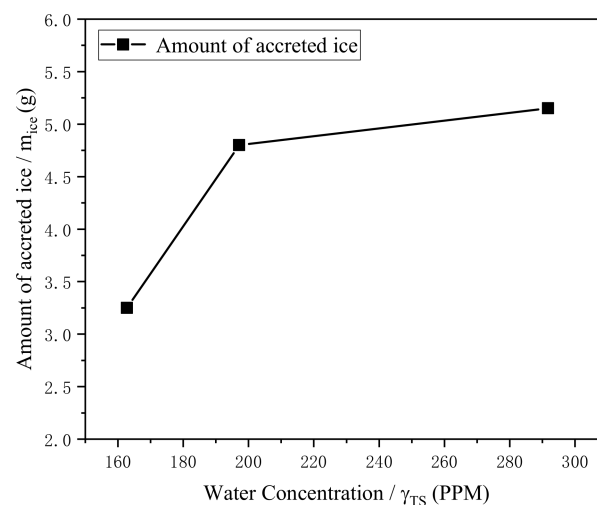


Figure 12. Mass of accreted ice in the upstream test section versus the water concentration.

4. Conclusions

When the fuel system encounters a cold environment, ice accumulation in the absence of additives is inevitable. The super-saturated fuel entrains water droplets/nucleation particles and flows in pipes in emergency conditions, leading to accreted ice. Hence, experiments were carried out to study accreted ice of super-saturated low-temperature fuel in the pipe. A method for preparing the quantitative water concentration of flowing fuel in a loop was presented, and the key parameters, such as test duration, fuel temperature, and water concentration, were analyzed.

There were two different depositions on the inner wall of the pipe: one was in the form of soft ice and the other was hard and exhibited a ‘pebbly’ appearance. The water solubility decreases exponentially with decreased fuel temperature, which promotes soft ice accumulation. The accreted ice exhibited a non-uniformity at the cross-sectional area

with the distance of flow. With respect to the test duration, the amount of ice accretion showed an increasing trend and became stable after 2 h. Besides, the amount of accreted ice increased with a decrease in the fuel temperature between $-2\text{ }^{\circ}\text{C}$ and $-12\text{ }^{\circ}\text{C}$. Part of the soft ice was shed off at fuel temperature $-15\text{ }^{\circ}\text{C}$. The amount of accreted ice increased with the increase in water concentration in the fuel.

We believe that our findings regarding the tendency of icing may serve as the basis for aircraft fuel system design and airworthiness certification.

Author Contributions: Conceptualization, C.Z. (Chengxiang Zhu) and J.W.; methodology, C.Z. (Chengxiang Zhu), Q.B., C.L., N.Z., and C.Z. (Chunling Zhu); formal analysis, C.Z. (Chengxiang Zhu) and J.W.; writing—original draft preparation, C.Z. (Chengxiang Zhu) and J.W.; writing—review and editing, N.Z. and C.Z. (Chunling Zhu); funding acquisition, C.Z. (Chengxiang Zhu), J.W., Q.B., C.L., N.Z. and C.Z. (Chunling Zhu). All authors have read and agreed to the published version of the manuscript.

Funding: This research was funded by the National Natural Science Foundation of China (11832012) and the Fundamental Research Funds for the Central Universities (NP2020402).

Data Availability Statement: The data presented in this study are available on request from the corresponding author. Informed consent was obtained from all subjects involved in the study.

Conflicts of Interest: The authors declare no conflict of interest.

Nomenclature

| | | | |
|----------------------|---|----------|----------------------|
| AAIB | Air Accidents Investigation Branch | | |
| FOHE | Fuel-Oil Exchanger | | |
| WBF | Wegener-Bergeron-Findeisen | | |
| EASA | European Aviation Safety Agency | | |
| FAA | Federal Aviation Administration | | |
| SST | Stainless Steel | | |
| M | Injection rate of micro syringe pump | | |
| V | Flow volume of fuel | | |
| γ_{TS} | Water concentration of fuel in the test section | | |
| γ | Water concentration of saturated fuel | | |
| U_{TS} | Velocity of fuel flow in the test section | | |
| Re | Reynolds number | | |
| v | Falling velocity of droplets in fuel | | |
| ρ_w | Density of droplets | ρ_f | Density of fuel |
| g | Gravity acceleration | d | Diameter of droplets |
| μ_f | Dynamics viscosity of fuel | T_f | Temperature of fuel |
| t | Test period | | |

References

1. CRC. *Handbook of Aviation Fuel Properties*, 3rd ed.; Technical Report, CRC Report No. 635; CRC: Boca Raton, FL, USA, 2004.
2. AAIB. *Report on the Accident to Boeing 777-236ER, G-YMMM, at London Heathrow Airport on 17 January 2008*; AAIB: Hampshire, UK, 2014.
3. Lao, L.; Ramshaw, C.; Yeung, H.; Carpenter, M.; Hetherington, J.; Lam, J.K.-W.; Barley, S. Behaviour of Water in Jet Fuel in a Simulated Fuel Tank. *SAE Tech. Paper* **2011**. [[CrossRef](#)]
4. Wu, N.; Zong, Z.; Hu, J.; Ma, J. Mechanism of dissolved water in jet fuel. *AIP Conf. Proc.* **2017**, *1820*, 040014.
5. Murray, B.; Broadley, S.; Morris, G. Supercooling of water droplets in jet aviation fuel. *Fuel* **2011**, *90*, 433–435. [[CrossRef](#)]
6. Lam, J.; Hetherington, J.; Carpenter, M. Ice growth in aviation jet fuel. *Fuel* **2013**, *113*, 402–406. [[CrossRef](#)]
7. Lam, J.; Lao, L.; Hammond, D.; Power, J.P. Character and Interface Shear Strength of Accreted Ice on Subcooled Surfaces Submerged in Fuel. *Aeronaut. J.* **2015**, *119*, 1377–1396. [[CrossRef](#)]
8. Maloney, T.C. *The Collection of Ice in Jet A-1 Fuel Pipes*; Rutgers The State University: New Brunswick, NJ, USA, 2012.
9. Maloney, T.C.; Diez, F.J.; Rossmann, T. Ice accretion measurements of Jet A-1 in aircraft fuel lines. *Fuel* **2019**, *254*, 115616. [[CrossRef](#)]
10. Schmitz, M.; Schmitz, G. Experimental study on the accretion and release of ice in aviation jet fuel. *Aerosp. Sci. Technol.* **2018**, *82–83*, 294–303. [[CrossRef](#)]

11. Lam JK, W.; Woods, R.D. Ice accretion and release in fuel systems: Large-scale rig investigations. *Aeronaut. J.* **2018**, *122*, 1051–1082. [[CrossRef](#)]
12. Johnson, J.U.; Carpenter, M.; Williams, C.; Pons, J.-F.; McLaren, D. Complexities associated with nucleation of water and ice from jet fuel in aircraft fuel systems: A critical review. *Fuel* **2022**, *310*, 122329. [[CrossRef](#)]
13. SAE International. Considerations on Ice Formation in Aircraft Fuel Systems, SAE AIR, 2006, 790C. Available online: <https://www.sae.org/standards/content/air790c/> (accessed on 18 November 2022).
14. SAE International. Aircraft Fuel System and Component Icing Test, SAE ARP, 2012 1401B. Available online: <https://www.sae.org/standards/content/arp1401b/> (accessed on 18 November 2022).
15. Lam, J.; Carpenter, M.; Williams, C.; Hetherington, J.I. Water solubility characteristics of current aviation jet fuels. *Fuel* **2014**, *133*, 26–33. [[CrossRef](#)]
16. Baena-Zambrana, S.; Repetto, S.L.; Lawson, C.P.; Lam, J.K.-W. Behaviour of water in jet fuel—A literature review. *Prog. Aerosp. Sci.* **2013**, *60*, 35–44. [[CrossRef](#)]
17. Lin, G.; Liu, D.; Wang, Y. Research on the Influencing Factors of Fuel System Pipe Icing of Transport Aircraft. *ISMSEE* **2022**, 1–4.
18. Chen, T.; Xu, X.; Hu, J.; Guo, L.; Yang, S.; Zhao, T.; Ma, J. Water behavior of current jet fuel versus operating conditions: Storage time, temperature, relative humidity and anti-icing agent. *Fuel* **2022**, *309*, 122088. [[CrossRef](#)]
19. Charro, A.; Baena, S.; Lam, J.K.W. Water Solubility in Different Alternative Jet Fuels: A Comparison with Petroleum-Based Jet Fuel. *SAE AeroTech Congr. Exhib.* **2015**. No.2015-01-2563.
20. West, Z.J.; Yamada, T.; Bruening, C.R.; Cook, R.L.; Mueller, S.S.; Shafer, L.M.; DeWitt, M.J.; Zabarnick, S. Investigation of water interactions with petroleum-derived and synthetic aviation turbine fuels. *Energy Fuels* **2018**, *32*, 1166–1178. [[CrossRef](#)]
21. Dang, Q.; Song, M.; Dang, C.; Zhan, T.; Zhang, L. Experimental study on solidification characteristics of sessile urine droplets on a horizontal cold plate surface under natural convection. *Langmuir* **2022**, *38*, 7846–7857. [[CrossRef](#)] [[PubMed](#)]
22. Work, A.; Lian, Y. A critical review of the measurement of ice adhesion to solid substrates. *Prog. Aerosp. Sci.* **2018**, *98*, 1–26. [[CrossRef](#)]
23. Archer, P.; Gupta, V. Measurement and control of ice adhesion to aluminum 6061 alloy. *J. Mech. Phys. Solids* **1998**, *46*, 1745–1771. [[CrossRef](#)]

Disclaimer/Publisher’s Note: The statements, opinions and data contained in all publications are solely those of the individual author(s) and contributor(s) and not of MDPI and/or the editor(s). MDPI and/or the editor(s) disclaim responsibility for any injury to people or property resulting from any ideas, methods, instructions or products referred to in the content.